JOURNAL OF MATERIALS SCIENCE **39** (2004) 5417– 5420

Deformation induced Nanostructure and texture in MP35N alloys

A. ISHMAKU, K. HAN*
National High Magnetic Field Laboratory, Florida State University, 1800 E. Paul Dirac Dr., Tallahassee, FL 32310, USA
E-mail: han@magnet.fsu.edu

The macro-texture was related to the nano-platelets formed during the rolling deformation of a Co-Ni-Cr-Mo alloy (MP35N) with low stacking fault energy. The deformed materials showed {011}⟨533⟩ texture but also had {011}⟨211⟩ and {011}⟨100⟩ texture components. The {011}⟨533⟩ component reached the maximum at 74% reduction-in-area. Further deformation of the material to 80% decreased the intensity of the {011}⟨533⟩ component. The cold deformation introduced platelets of a few atomic layer in thickness and less than 100 nm in diameters. The habit planes of the platelets were identified to be {111}, which were perpendicular to both the rolling and {011} crystallographic plane. Therefore, the tensile strain in the rolling direction assisted formation of the platelets, which were identified as stacking faults. A high density of nano-platelets and dislocations strengthened materials and influenced the plastic deformation behaviors and texture evolution. Thus, the MP35N developed slightly different textures from other low stacking fault energy materials. The maximum at {011}⟨533⟩ was related the nanoplatelets and stacking fault energy. The {011}⟨112⟩ and {110}⟨001⟩components could be linked to the low stacking fault energy.

1. Introduction

MP35N alloy was studied as one of the face-centered cubic structure materials suitable for application at cryogenic temperatures, and in particular as one of the reinforcement materials for high pressure applications. The high strength MP35N can be manufactured by cold rolling, which introduces texture in the materials. It was reported that metals with low or high stacking fault energy (SFE) usually had brass ({011}⟨112⟩) or copper-type ({112}⟨111⟩) texture components, respectively [1]. However, some low SFE materials may have a texture component different from brass-type. For instance, the cold rolled low oxygen silver (with low SFE energy) was reported to have a deformation texture with maxima at {110}⟨335⟩ [2]. Therefore, it is necessary to investigate the individual material in order to characterize the texture. Some studies on texture in MP35N were performed by transmission electron microscopy [3] and X-Ray Diffraction (XRD) [4]. The XRD results demonstrated that the global texture of MP35N was {110}⟨112⟩ and {110}⟨111⟩ after the materials were cold-rolled [4]. However, the texture analysis has not been related to the deformation strain yet. The cold-rolling also introduced very fine platelets nucleating on one set of {111} planes. The fine platelets strengthen the face-centered-cubic (fcc) matrix. The present work focuses on the texture evolution of MP35N during the deformation. In addition, the habit planes and sizes of the nanoplatelets are also related to the texture in the materials.

2. Experimental procedure

The samples of the MP35N sheets were received in the cold-rolled form from CSM Industries Inc. The typical composition is 33.24 wt%Co-35.72 wt%Ni-19.93 wt%Cr-9.61 wt%Mo. The MP35N rolled to 65, 74 and 80% had the thickness of 0.077, 0.106, and 0.16 mm respectively.

The crystallographic textures of the sheets were determined in the area about 8 cm from the sheet center by measuring pole figures in reflection geometry using X'Pert Materials Research Diffractometer system with a point focus configuration and Ni-filtered Cu K_α radiation. In order to exclude the influence of possible texture gradients close to the surface of the specimens, the surface layers were carefully removed by polishing and etching. For quantitative macro-texture analysis, the orientation distribution function (ODF, f(g)), was calculated from three incomplete {111}, {200}, {220} pole figures by the X'Pert Texture software based on the Williams-Imhof-Matthies-Vinel method after correction of background and defocus [5]. Fine grids of $3^\circ \times 3^\circ$ in rotation Phi and tilt Psi angles were chosen to measure the pole figures [5]. The ODF was calculated and presented by Bunge convention of Euler angles [5].

*Author to whom all correspondence should be addressed.

The range of the angles in ODF was $0 \leq$ (Phi1, PHI, Phi2) ≤ 90.

Discs 3 mm in diameter were sectioned from the MP35N sheets for TEM examination. The discs were polished using a Fishione Instruments Model 110 Twin-Jet Electropolisher. The electrolyte contained 19 vol% H_2SO_4, 76 vol% methanol and 5 vol% H_3PO_4. The electropolisher was operated at a current of 28–32 mA, and temperature of 3–5°C. The foils were examined with a Jeol Jem-2010 electron microscope operated at 200 kV.

3. Results

In all the specimens, the maxima of the texture are found at angles PHI = 45° and Phi2 = 0°. The differences of the maxima position are at Phi1. Therefore, in Fig. 1a–c, the ODF diagrams are shown at Phi2 = 0° in order to elucidate the major texture evolution of MP35N cold rolled to 65, 74 and 80% reductions, respectively. The maxima of the texture are at Phi1 of 42°, 39°, and 39° respectively, for samples cold-rolled to 65, 74 and 80% reductions, respectively. All the orientation densities are concentrated at the main α-fiber, which extends from Goss component (011)[100] at Phi1 = 0°, PHI = 45°, through the brass component (011)[2$\bar{1}$1] to the maxima (011)[5$\bar{3}$3] at Phi1 between 39–42°, PHI = 45°. Therefore, the cold-rolling process maximized the number of {011} planes that are parallel to the sheet surface. The variation of the texture on {011} can be seen more clearly in Fig. 2a showing the orientation density values along the α-fiber of MP35N cold-rolled for different reductions. As deformation proceeds, the intensity at α fiber is retained, and the intensity distributions of the three samples are similar. At the reduction-in-area of 74%, the texture appears to reach the maximum intensity. This can also be seen by comparison of the half-value of maximum width of the α-tube, which are 39°, 33°, and 39° for samples deformed to 65, 74, and 80% respectively. Therefore, the texture sharpens with increasing rolling reduction from 65 to 74% and then becomes weaker when the materials are rolled to 80%.

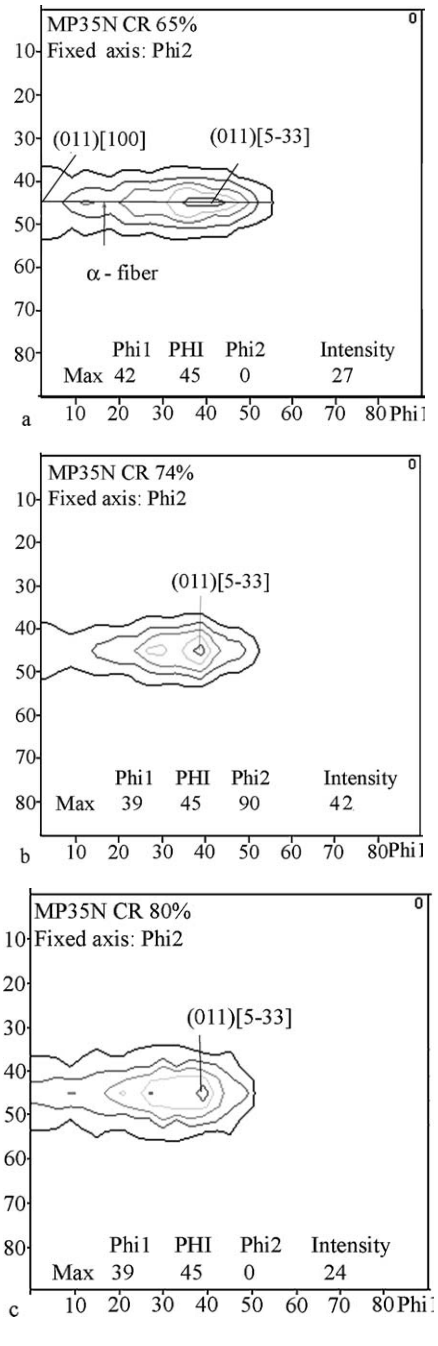

Figure 1 The ODF at Phi2 = 0° of MP35N cold-rolled to (a) 65%, (b) 74%, (c) 80% reduction-in-area. In figure (a), a line was drawn to show how the α-fiber (Fig. 2a) was constructed.

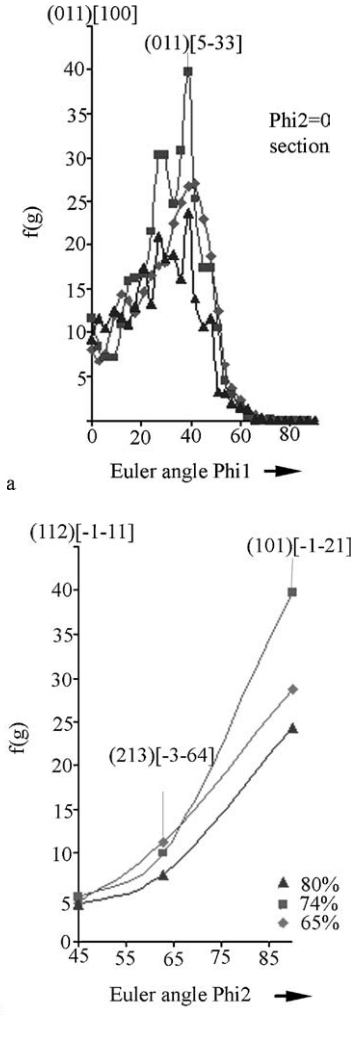

Figure 2 Intensity changes along various fibers in MP35N deformed to different reduction: (a) the α-fiber and (b) the β-fiber.

Figure 3 Transmission electron microscopy image showing nanoplatelets nucleated on {111} habit planes in MP35N.

Fig. 2b shows the orientation density of the copper ({112}⟨111⟩), S ({123}⟨634⟩) and brass ({110}⟨112⟩) components and along the β-fiber. The figure demonstrates that the brass component is the strongest one among all the three components and the copper (112)[$\bar{1}\bar{1}$1] is the weakest one.

As the {011} is the most important crystallographic planes in this material, all the TEM examinations were undertaken with the sample normal in {011}. Two of the most important observations are (1) very fine mechanical twins formed in the materials in the selected area and (2) nucleation of the nanoplatelets on {111} planes, as shown in Fig. 3, which presents a typical image of MP35N rolled to 65%. The habit planes are perpendicular to {011} and 60 degrees from the rolling direction [5$\bar{3}$3]. The sizes of the platelets are less 100 nm in diameter, and less than 1 nm in thickness. The distance between the platelets is about 50 nm.

4. Discussion

The plane strain deformation, which has a compressive strain in the direction of the sheet normal (ND), which is the {011} of the crystallographic plane, a tensile strain in the rolling direction (RD) and almost no strain in the transverse direction (TD), induces a strong texture in MP35N alloy. Most of the intensities lie along α-fiber shown in Figs 1 and 2a. The strongest component at the maximum intensity can be expressed both in direction cosines and the nearest family of Miller indices: (0 0.707 0.707)[0.743 $\overline{0.473}$ 0.473] $\rightarrow$ (011)[5$\bar{3}$3] at Phi2 = 0°, (0.707 0 0.707)[$\overline{0.500}$ $\overline{0.777}$ 0.500] $\rightarrow$ (101)[$\bar{3}\bar{5}$ 3] at Phi2 = 90°, (0 0.707 0.707)[0.777 $\overline{0.445}$ 0.445] $\rightarrow$ (011)[5$\bar{3}$3] at Phi2 = 0° for samples deformed to 65, 74, and 80% reduction, respectively. Therefore, the rolling results in the majority of single crystals rotating towards {011}⟨533⟩ orientation and shear in the direction of ⟨112⟩. Such a deformation promotes the formation of the nano-platelets on {111} planes in the materials. Further deformation from 65% causes the compression normal to the rolling plane {011}, and elongation in the rolling direction (with majority of the grains in ⟨533⟩) without significant alternation of the orientation of the major texture. It is also noticed that the Cu component is relatively weak. Such an orientation distribution invokes a strong evidence that materials have a low stacking fault energy (γ_{SFE}) similar to brass 70/30, brass 80/20, 316 types of stainless steels and silver which have γ_{SFE} of 7, 9, 14 [6], and 24 [7] mJ/m^2 respectively.

However, the maximum showed at {110}⟨335⟩ orientation in MP35N with γ_{SFE} of 13 mJ/m^2 [6], is slightly different from that of some low stacking fault energy materials, such as brass. This can be related to the deformation behavior of this high strength material with fcc crystallographic structure. The major difference between this material and other low SFE metallic materials, such as brass, is the modulus and yield strength. In addition, this material is strengthened significantly by very fine platelets, whereas in other low SFE materials,

stacking faults or twins with relatively large thickness form during the deformation. The high yield strength of this material results in the plastic deformation to occur at relatively larger stresses than other low SFE materials, but the high modulus causes the materials deform at relatively small strain. The large stress and low strain appear to result in more homogeneous shear deformation than other low SFE materials, so that very fine platelets similar to stacking faults nucleate on $\{111\}_{fcc}$ planes instead of the large deformation twins. Within a single grain, the nanoplatelets are parallel to each other and the distance between them is from a few nanometers to 50 nanometers. Although the platelets are only a few atomic layers in thickness, they facilitate a homogeneous deformation at even higher stresses than yield strength of annealed materials. The platelets therefore supply a strong barrier to the dislocation motion, and consequently our mechanical test data demonstrate that the strength of the deformed materials reaches 2 GPa or higher. The platelets also limit the slip of $\{111\}\langle 110\rangle$ so that very large strain hardening is possible even at stress level more than 1000 MPa. Such a high strength level resulting from the nanoplatelets makes the $\{111\}\langle 112\rangle$ types shear difficult, so that the $[5\bar{3}3]$ orientation is parallel to the rolling direction. However, such an orientation still makes the $\langle 110\rangle$ double slip possible so that formation of the high density of $\langle 110\rangle$ type dislocation on $\{111\}$ occurs as observed by TEM.

Significant amount of annealing twins occur in the materials before deformation. Examinations of the microstructure using various microscopy show that cold-rolling introduces rotation of annealing twins in the MP35N fcc matrix in order to align the twin boundary parallel to the rolling direction and accommodate the $\{111\}$ slip planes in both matrix and twins. The twin planes appear to deviate from $\{111\}$ due to the heavy deformation so that irrational annealing twin planes were observed. The rotation of the annealing twins is accompanied by the formation of the nanoplatelets and the material becomes stronger. Therefore, further rotation is more difficult. The material is stabilized with $\langle 533\rangle$ parallel to the rolling direction.

5. Conclusions

The MP35N alloy shows the major texture components distributing at the α-fiber starting from $\{011\}\langle 100\rangle$, through $\{011\}\langle 211\rangle$ to the maxima $\{011\}\langle 533\rangle$ after being cold rolled up to 80%. The $\{112\}\langle 111\rangle$ component nearly disappears, because of low SFE. Along with the development of the texture, nanoplatelets form on $\{111\}$ habit planes which are perpendicular to the $\{011\}$ and about 60 degrees from $\langle 533\rangle$.

Acknowledgment

Financial support from the National High Magnetic Field Laboratory, Florida State University is gratefully acknowledged. We also thank Mrs. Cristiane Bacaltchok and Dr. Yan Xin for assistance in doing some experiments, and Dr. Garmestani for supplying the Philips Analytics facilities, Mr. Edwards in CSM Industries for supplying the materials and performing some tensile tests.

References

1. R. E. SMALLMAN and D. GREEN, *Acta Metall.* **12** (1964) 145.
2. T. A. GLADSTONE, J. C. MOORE, B. M. HENRY, S. SPELLER, C. J. SALTER, A. J. WILKINSON and C. R. M. GROVENOR, *Supercond. Sci. Technol.* **13** (2000) 1399.
3. S. ASGARI, E. EL-DANAF, S. R. KALIDINDI and R. D. DOHERTY, *Metall. Mater. Trans.* A **28** (1997) 1781.
4. A. ISHMAKU and K. HAN, *Mater. Charact.* **47** (2001) 139.
5. V. RANDLE and O. ENGLER, "Introduction to Texture Analysis, Macrotexture, Microstructure and Orientation Mapping" (Gordon and Breach Science Publishers, 2000) p. 75, p. 103, p. 104.
6. E. EL-DANAF, S. R. KALIDINDI and R. D. DOHERTY, *Metall. Mater. Trans.* A **30** (1999) 1227.
7. P. C. GALLAGHE, *Metall. Trans.* **1** (1970) 2429.

Received 11 September 2003
and accepted 27 February 2004